Synchronization of spatiotemporal chaos and its applications

Gang Hu,[1,2] Jinghua Xiao,[3] Junzhong Yang,[2] Fagen Xie,[4,5] and Zhilin Qu[2,5]
[1]*China Center of Advanced Science and Technology (CCAST), P.O. Box 8730, Beijing 100080, China*
[2]*Physics Department, Beijing Normal University, Beijing 100875, China*
[3]*Department of Basic Science, Beijing University of Posts and Telecommunications, Beijing 100088, China*
[4]*Institute of Theoretical Physics, Academia Sinica, Beijing 100080, China*
[5]*Department of Medicine, Division of Cardiology, University of California, Los Angeles, California 90095*
(Received 15 April 1997)

Synchronization of spatiotemporal chaos is investigated, based on the models of one-way coupled map lattice systems. It is found that under certain conditions spatiotemporal hyperchaos with a huge number of positive Lyapunov exponents can be synchronized by simply driving a single site, and the mechanism for this efficiency is analyzed. This approach of spatiotemporal chaos synchronization is applied for multichannel secure communication and secure information storage. [S1063-651X(97)07609-5]

PACS number(s): 05.45.+b, 89.70.+c

I. INTRODUCTION

In recent years the investigation of chaos control and synchronization has attracted much attention [1–13]. This investigation is an important step towards applications of chaos. A further and natural development in this respect goes to control and synchronization of spatiotemporal chaos [14–21]. There are some great advantages of spatiotemporal chaos in comparison with low-dimensional chaos. For instance, when we apply chaos for treating information, in the former case there exist a huge number of spatial sites, each of which takes chaotic motion and serves as an information operator, and then the information operations can be performed simultaneously and parallelly by many subunits if one can properly drive and control extended systems, and thus the efficiency of information treatment can be significantly enhanced. The potential for the applications of spatiotemporal chaos control and synchronization is extremely great and unlimited. In this paper we will show how one can synchronize two identical spatiotemporal systems consisting of a huge number of coupled spatial sites by driving only a single site for each system, and how this synchronization of chaos can be used for multichannel secure communication and spatial information storage. This paper is developed from our early paper [21], and contains some essentially additional results in the treatment of spatially two-dimensional coupled systems.

II. SYNCHRONIZATION OF SPATIOTEMPORAL CHAOS

Let us start with the following one-dimensional (1D) one-way coupled ring map lattice of length L (OCRML-L) [22,23]

$$z_{n+1}(i)=(1-\varepsilon)f(z_n(i))+\varepsilon f(z_n(i-1)),$$
$$z_n(i+L)=z_n(i), \tag{2.1}$$

where $i=1,2,\ldots,L$ is the lattice site index, n is the time index, ε the coupling constant, and $f(x)$ is taken to be some nonlinear function. Here we use the logistic map $f(x)=ax(1-x)$, which has, as a single map, a period-doubling cascade with the accumulation point at $a_c=3.569\,9456,\ldots$ and chaos can be found in the interval $a_c<a<4$. When $a=4$ (we will always take $a=4$ for the investigation throughout the paper) $f(x)$ maps the interval $[0,1]$ into itself and the single site system is now in a fully developed chaotic state. One can easily verify that after applying couplings the OCRML system is chaotic except in a small coupling interval about $0.16\leqslant\varepsilon\leqslant 0.19$. In Fig. 1 we fix $\varepsilon=0.85$, an obvious fully developed spatiotemporal chaos (chaotic in time and random in space) can be observed.

The ring of Eqs. (2.1) can be cut to produce a one-way-coupled open map lattice (OCOML)

$$x_{n+1}(i)=(1-\varepsilon)f(x_n(i))+\varepsilon f(x_n(i-1)),\quad i=2,3,4,\ldots,$$
$$x_n(1)=s_n, \tag{2.2}$$

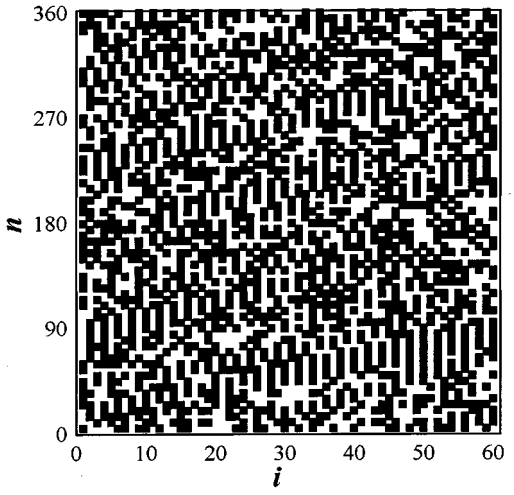

FIG. 1. A fully developed spatiotemporal chaos of Eqs. (2.1). $a=4$, $\varepsilon=0.85$, $L=60$. Pixels are painted black as $x_n(i)\geqslant 0.75$, and left blank otherwise.

where the period boundary condition of Eqs. (2.1) is replaced by the open flow condition. Now the lattice length L has no meaning for Eq. (2.2) because the open boundary gives no feedback to the motions of the previous system sites. In the OCOML system the first site $x_n(i=1)$ is in a special position, and its variation is externally given. Then this externally injected sequence $x_n(1)=s_n$ provides a natural way of control.

Equations (2.2) have two important and useful properties. First, all solutions of Eqs. (2.1) belong to the solutions of Eqs. (2.2) with a proper driving s_n. Suppose $z_n(1), z_n(2), \ldots, z_n(L)$ are the sequences produced by Eqs. (2.1): by injecting

$$x_n(1)=s_n=z_n(j), \tag{2.3a}$$

the spatially periodic sequences

$$\begin{aligned} &x_n(2)=z_n(j+1),\\ &x_n(3)=z_n(j+2),\ \ldots,x_n(L-j)=z_n(L),\\ &x_n(L-j+1)=z_n(1),\ \ldots,x_n(L)=z_n(j-1),\\ &x_n(kL+i)=x_n(i),\quad k=1,2,\ldots \end{aligned} \tag{2.3b}$$

must be a solution of Eqs. (2.2). Then, the spatiotemporal solution of Fig. 1 [an asymptotic solution of Eqs. (2.1)] must be a solution of Eqs. (2.2) if we take the chaotic sequence of an arbitrary site $z_n(j)$ as the driving sequence of Eq. (2.3a). Second, at $\varepsilon>0.75$ Eqs. (2.2) have only a unique asymptotic state for any given driving sequence. Let us suppose another coupled system:

$$\begin{aligned} &y_{n+1}(i)=(1-\varepsilon)f(y_n(i))+\varepsilon f(y_n(i-1)),\\ &y_n(i=1)=s_n=x_n(i=1), \end{aligned} \tag{2.4}$$

identical to Eqs. (2.2). However, the initial conditions of Eqs. (2.2) and Eqs. (2.4) may be different. Now we consider the evolution of the difference $y_n(i)-x_n(i)$, $i=2,3,\ldots$. From Eqs. (2.2) and Eqs. (2.4) we obtain

$$\begin{aligned} |y_{n+1}(2)-x_{n+1}(2)| &= (1-\varepsilon)a|y_n(2)-x_n(2)|\\ &\quad\times|y_n(2)+x_n(2)-1|\\ &< (1-\varepsilon)a|y_n(2)-x_n(2)| \end{aligned}$$

as $\varepsilon>0.75$ we have

$$\begin{aligned} &|y_{n+1}(2)-x_{n+1}(2)|<\lambda|y_n(2)-x_n(2)|,\\ &0<\lambda=(1-\varepsilon)a<1 \end{aligned} \tag{2.5}$$

leading to $\lim_{n\to\infty}[y_{n+1}(2)-x_{n+1}(2)]=0$. Repeating the same computations we can prove successively

$$\lim_{n\to\infty}[y_{n+1}(i)-x_{n+1}(i)]=0,\quad i=3,4,\ldots,N,\ldots. \tag{2.6}$$

Therefore, Eqs. (2.2) have a single asymptotic solution, which is completely determined by the driving force s_n. All initial conditions of Eqs. (2.2) will be eventually forgotten during the evolution. It shows that at $\varepsilon>0.75$, the system (2.2) is completely controllable by the driving s_n. Combining the above two properties we can conclude that at $\varepsilon>0.75$ all solutions of Eqs. (2.1) (whether they are stable or unstable in the original OCRML system) are stable and unique asymptotic solutions of Eqs. (2.2), for the given drivings Eqs. (2.3a), and spatiotemporal chaos of Eqs. (2.2) and (2.4) can be completely synchronized to the solution of Eqs. (2.1) by the driving (2.3a) whatever the initial conditions of these two systems. We have tried numerical simulations of two identical lattices, each consisting of 5000 sites. The synchronization of two identical systems from different initial conditions is perfectly verified. This synchronization will be shown to be extremely useful for the applications of spatiotemporal chaos.

III. MULTICHANNEL SECURE COMMUNICATION BY SYNCHRONIZING SPATIOTEMPORAL CHAOS

We first consider the application of secure communication by synchronizing spatiotemporal chaos. Recently, secure communication by chaos synchronization has become a hot topic [8–10,21,24–26]. An information signal containing a message can be transmitted by using a chaotic signal as a broadband carrier, and synchronization of chaos can be used to recover the information at the receiver. The advantages of this sort of secure communication have been repeatedly emphasized. However, most investigations have focused on the problem of secure communication by using low-dimensional chaotic systems as transmitters and receivers where only a single or very few signal transmission channels are available.

Now we investigate the possibility of making multichannel secure communication by synchronizing spatiotemporal chaos. The communication efficiency can be greatly enhanced since a large number of informative signals can be transmitted and received simultaneously. To fulfill this task the operating spatiotemporal systems must have the following properties. (i) The chaotic motions of two identical systems can be synchronized by using control keys as few as possible. The most convenient situation is that these spatiotemporal chaotic motions can be synchronized by using a single key. (ii) The chaotic signals transmitted from different channels must be independent of (or uncorrelated with) each other; then the interferences between different transmitted signals can be reduced to the lowest level. (iii) It is better that the key sequences and the transmitted chaotic signals are high-dimensional hyperchaos so that any imitations of keys and attacks against the transmitted signals are extremely difficult.

From the analysis of Sec. II, we found that the above first requirement can be perfectly met by systems (2.2) and (2.4), where synchronization of spatiotemporal chaos can be definitely achieved by using a single key s_n as $\varepsilon>0.75$. Actually, $\varepsilon>0.75$ is a sufficient while not a necessary condition for synchronization of chaos. In Fig. 2(a) we numerically test the necessary condition for this chaos synchronization. For a given pair of L and ε, we run the OCRML system (2.1) and take out a chaotic signal $z_n(i)$ from a cell chosen arbitrarily. Then we use this extracted chaotic sequence as a key to control the systems (2.2) and (2.4) by setting $x_n(1)=y_n(1)=s_n=z_n(i)$ and keeping ε unchanged, and study whether the

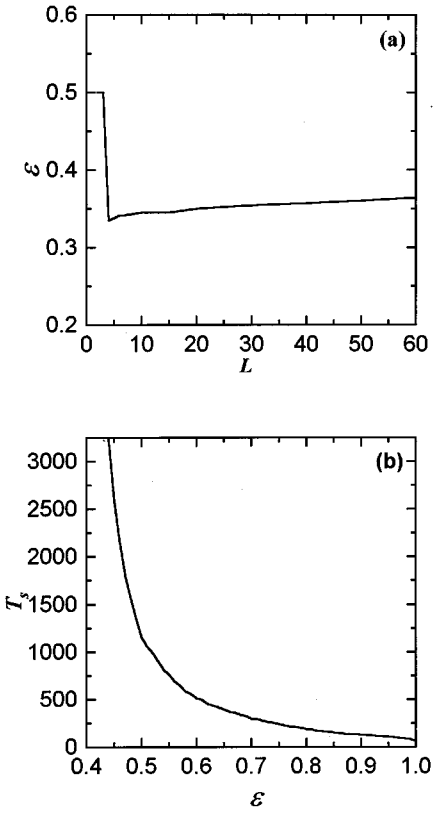

FIG. 2. (a) ε plotted vs L where L is the lattice size of the OCRML system (2.1) from which the driving sequence is extracted. Above the ε-L curve, spatiotemporal chaos of identical OCOML systems (2.2) and (2.4) can be synchronized after 10^5 iterations whatever the initial conditions for $i=2,3,\ldots$. (b) $L=60$, the synchronization time T_s vs ε.

two OCOML systems can be synchronized. For any given L of OCRML we find a critical $\varepsilon_c(L)$ indicated by the curve of Fig. 2(a), where for $\varepsilon<\varepsilon_c(L)$ no synchronization can be achieved. For $\varepsilon>\varepsilon_c(L)$ we can successfully achieve synchronization of chaos. It is striking that the coupling threshold for synchronizing chaos depends on different chaotic driving. The threshold is saturated to a value about $\epsilon=0.37$ as $L\to\infty$, which is much smaller than 0.75. The quantity of synchronization time T_s is important in practice. In Fig. 2(b) we fix $L=60$ and plot T_s against ε with T_s being defined as the time needed to fulfill

$$\Delta=\frac{1}{L}\sum_{i=1}^{L}[y_n(i)-x_n(i)]^2<10^{-16}$$

for any $n>T_s$, where $y_n(i)$ and $x_n(i)$ are the outputs of the first 60 cells of the two identical OCOMLs. We get a monotonously decreasing curve. The behavior $T_s\to\infty$ as $\varepsilon\to\varepsilon_c$ is consistent with all the above discussions.

For secure communication, the identical extended systems (2.2) and (2.4) may serve as the transmitter and the receiver, respectively. The chaotic sequences of various space units $x_n(i)$, $i=2,3,\ldots$, may serve as multiple message carriers for the information transmission. Then the above condition (ii) that any two chaotic sequences from different transmission channels should be independent of (uncorrelated with) each other is of crucial importance for the multichannel communication. In Fig. 3 we fix $\varepsilon=0.95$ and plot various correlation quantities. In Fig. 3(a) we plot an autocorrelation of a chaotic signal versus time with

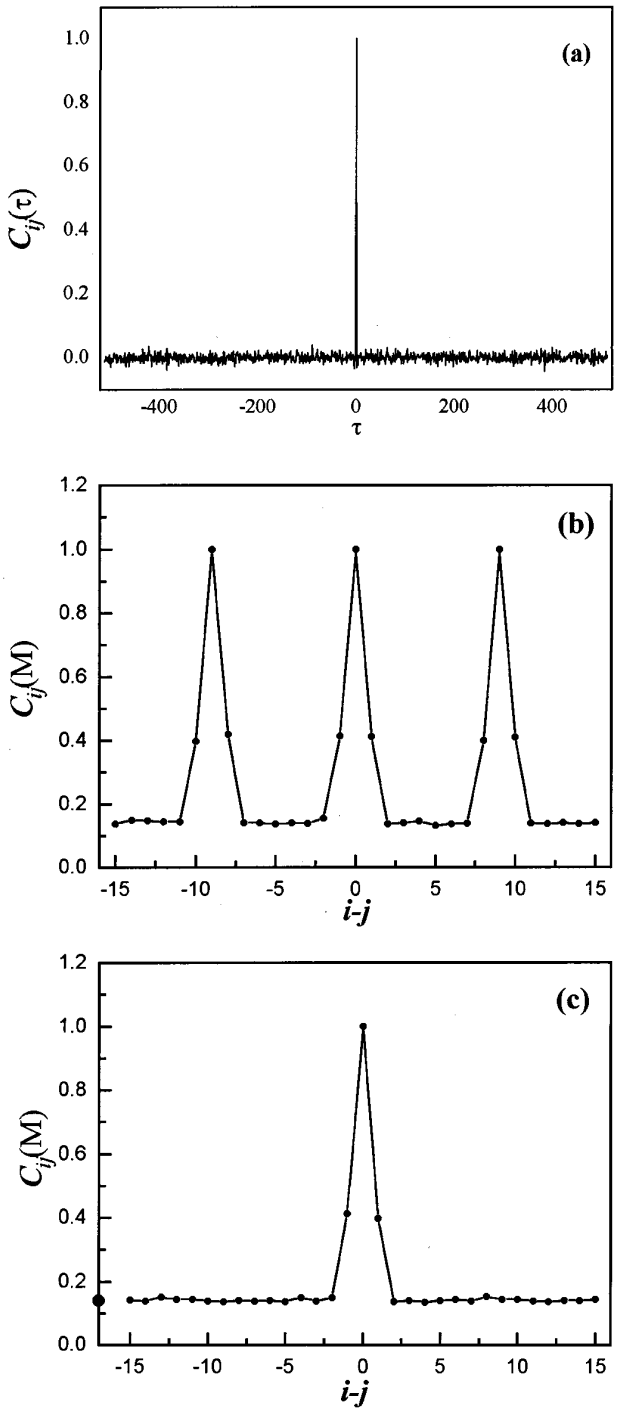

FIG. 3. $a=4$, $\varepsilon=0.95$, $L=9$, $T=512$ in Eqs. (2.1). (a) The autocorrelation $C_{ii}(\tau)$ vs τ. (b) The cross correlation $C_{ij}(M)$ vs $i-j$, where $C_{ij}(M)$ is the maximum of $C_{ij}(\tau)$ with respect to τ. The spatial periodicity of period-9 is due to the driving (extracted from OCRML-9). (c) The same as (b) with driving replaced by a random force uniformly distributed in [0,1]. The black disk is the mutual correlation of two independent random number sequences uniformly distributed in [0,1] with the same length $T=512$.

$$C_{ii}(\tau)=\hat{C}_{ii}(\tau)/\hat{C}_{ii}(0),$$

$$\hat{C}_{ii}(\tau)=\frac{1}{T}\sum_{n=1}^{T}[x_n(i)-x_A(i)][x_{n+|\tau|}(i)-x_A(i)], \tag{3.1}$$

$$|\tau|\in[0,T], \quad T=512,$$

where $x_A(i)$ is the average value of $x_n(i)$. T will be used to represent the characteristic time for variations of slowly varying informative signals. Each datum is obtained by averaging the results of 15 runs. A high peak of $C(\tau)$ is centered at $\tau=0$, and $C(\tau)$ damps very quickly to a very small value as $|\tau|$ increases. The δ-function-like time correlation (i.e., the widely spread spectrum distribution of the correction sequence) is favorable for spread-spectrum secure communication [26–28]. The quantity of normalized mutual correlation,

$$C_{ij}(\tau)=\hat{C}_{ij}(\tau)/\sqrt{\hat{C}_{ii}(0)\hat{C}_{jj}(0)}, \tag{3.2}$$

$$\hat{C}_{ij}(\tau)=\frac{1}{T}\sum_{n=1}^{T}[x_n(i)-x_A(i)][x_{n+|\tau|}(j)-x_A(j)],$$

is of practical importance for multichannel communication. In Fig. 3(b) we plot $C_{ij}(M)$, the maximum $C_{ij}(\tau)$ with respect to τ, versus $i-j$. It is extremely interesting that, apart from the nearest sites, sequences from two distinct sites are completely uncorrelated, in the sense that their cross correlation is practically the same as that of two independent random numbers uniformly distributed in [0,1] with the same length T [see the black disk in Fig. 3(c)]. Then, in the multichannel communication, the interferences between different transmitted sequences can be reduced to the lowest level. The spatial periodicity of period L in Fig. 3(b) is due to the fact that the chaotic driving is taken from an OCRML-L system. Actually, synchronization of Eqs. (2.2) and (2.4) can be also achieved by using an arbitrary random driving. In Fig. 3(c) we use a random sequence uniformly distributed in [0,1] as a driving force to substitute $x_n(1)$, and plot the same quantity as Fig. 3(b). $C_{ij}(M)$ is again very quickly dropping as $|i-j|$ increases, and the spatial periodic structure in Fig. 3(b) no longer exists for random driving.

For communication safety and robustness, one should forbid imitation of keys and avoid attacks against transmitted signals (i.e., avoid the interference of external signals correlated with the transmitted signals). For this purpose hyperchaos has a great advantage. We discuss this qualitatively. Suppose, for one-dimensional chaos, the probability of the imitation of keys and destruction of transmitted signals is $1/R$, $R\gg 1$. Then for a H-dimensional ($H>1$) hyperchaos this probability can be reduced to $(1/R)^H$. In Fig. 4 we fix $a=4$, $\varepsilon=0.95$, and run Eqs. (2.1), and then plot the number of positive Lyapunov exponents against the system size L. It is obvious that the dimension of the spatiotemporal chaos attractor of Eqs. (2.1), and consequently, the dimensions of the key and the transmitted signals, are very high for large L. It is practically impossible to imitate keys, and produce external chaotic sequences correlated with the transmitted signals for attacking the message carriers without knowing the exact information.

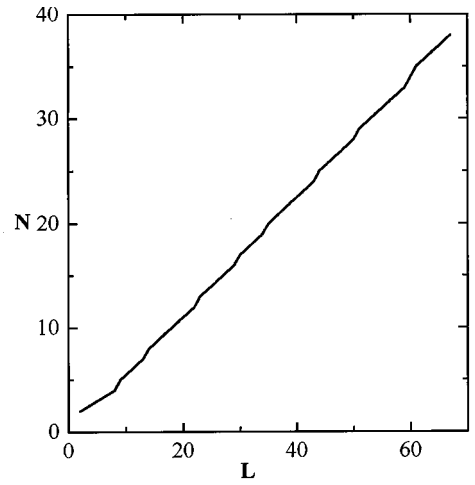

FIG. 4. The number of positive Lyapunov exponents of Eqs. (2.1), N, plotted vs the system size, L. N is proportional to L for large L. $a=4$, $\varepsilon=0.95$.

Based on the above features of the OCOML systems, we can now design multichannel secure communication equipment. Both transmitter and receiver are made by an identical OCOML system (specifically, we fix $\varepsilon=0.98$ for numerical simulations), and the active transmission channels can be appointed as $i=3,5,7,\ldots,2N+1$ for avoiding the mutual correlation between nearest sites. The transmitter extracts the key by running the corresponding OCRML-L system (2.1), and gives this key to the receiver before signal transmissions. The transmitter and the receiver can surely achieve synchronization of spatiotemporal chaos by using this identical key, starting from arbitrary initial conditions. The system length of the OCRML-L should be chosen sufficiently large so that there are enough mutually uncorrelated channels available for signal transmissions.

Then the transmitter uses its key to drive the OCOML system (2.2) to produce chaotic motions through the active channels. Suppose $x_n(i)$ is the chaotic sequence produced by the transmitter through the ith channel. Each datum of this sequence can be digitized and quantized to a subsequence of J number S_k, $k=1,2,\ldots,J$, of which each takes value $+1$ or -1 as

$$0<\left|x_n(i)-\sum_{k=1}^{J}[S_{n(k)}(i)+1]\left(\frac{1}{2}\right)^{k+1}\right|<\left(\frac{1}{2}\right)^{k}. \tag{3.3}$$

Suppose the sequence $S_{n(k)}$ represents the sequence $x_n(i)$ subject to quantization and digitization. For instance, as $x_n(i)=0.8$, for $J=5$ we have the subsequence $S_{n(1)}(i)=1$, $S_{n(2)}(i)=1$, $S_{n(3)}(i)=-1$, $S_{n(4)}(i)=-1$, $S_{n(5)}(i)=1$. Increasing J may effectively increase the accuracy of information transmission. The $(-1,1)$ quantization can greatly simplify the signal transmission procedures in realistic applications. This chaotic signal is modulated by an informative signal as $G_{n(k)}(i)=M_\nu(i)S_{n(k)}(i)$, where $M_\nu(i)$ is a sequence of numbers -1 and 1, the period for the possible variation of $M(i)$ is T with $T\gg 1$. The total time sequence

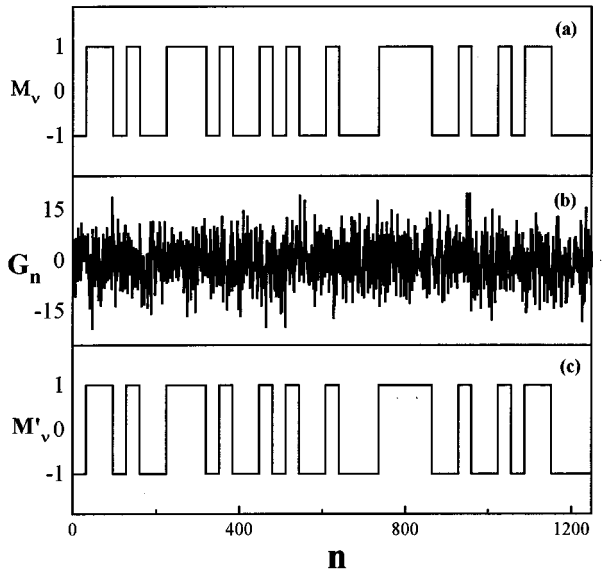

FIG. 5. (a) One of 39 modulation signals $M_v(i=21)$. (b) The mixture of 39 modulated chaotic signals subject to noise of 18 dB. $G_{n(k)}$ is obtained by running (2.1) with $a=4$, $\varepsilon=0.95$, and $L=84$. (c) The recovered modulation $M'_v(i=21)$, which is exactly identical to that of (a). Note that M'_v is set to 1 and -1 for $M'_v>0$ and <0, respectively.

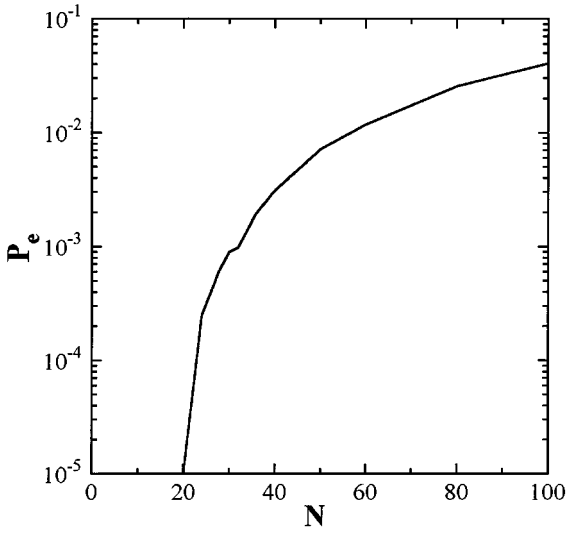

FIG. 6. Bit error probability P_e plotted vs the channel number N. $\varepsilon=0.98$, $T=32$, $J=10$.

received by the receiver is $G_{n(k)}=\Sigma_{\mu=1}^{N}G_{n(k)}(i=2\mu+1)$. The receiver can use the same key to drive the identical OCOML system (2.4), and produce the same chaotic sequence $S_{n(k)}(i)$, $i=3,5,\ldots,2N+1$. Then, the informative message can be recovered in the receiver by correlation checking as

$$\frac{1}{T}\sum_{n=\nu T+1}^{\nu T+T}\sum_{k=1}^{J}S_{n(k)}(i)G_{n(k)}\propto M_\nu(i). \tag{3.4}$$

All other signals in G_n are practically wiped out because $S_{n(k)}(i')$, $i'\neq i$, are not correlated to $S_{n(k)}(i)$. From Fig. 5 one can get some impression about various signals. Figure 5(a) shows 1 of 39 modulation signals $M_\nu(i=21)$; (b) gives the mixture of 39 modulated chaotic sequences G_n subject to a noise of 18 dB, from which no trace of signal can be seen. In (c) we recover $M_\nu(i=21)$ exactly by correlation checking (3.4). Figure 6 shows the efficiency of multichannel communication. P_e represents the bit error probability, where we fix $T=32$, $J=10$, and plot P_e against the channel number N. The error probability is lower than 10^{-3} even as the total number of signals in the mixture G_n becomes as large as 38. In Fig. 6, we use a rather small T. The bit error probability can be further reduced by increasing T. Therefore, multichannel secure communication is successfully performed by synchronizing spatiotemporal chaos. The communication efficiency can be greatly enhanced since a large number of informative signals can be transmitted simultaneously by using a single key.

IV. INFORMATION STORAGE AND RECOVER BY SYNCHRONIZING SPATIOTEMPORAL CHAOS

In Sec. III we used synchronization of spatiotemporal chaos of one-dimensional OCOML to perform multichannel secure communication. We can also use two-dimensional OCOML for the same purpose. A typical 2D OCOML can be defined as follows:

$$x_{n+1}(i,1)=(1-\varepsilon_1)f(x_n(i,1))+\varepsilon_1 f(x_n(i-1,1)),$$

$$x_{n+1}(1,j)=(1-\varepsilon_2)f(x_n(1,j))+\varepsilon_2 f(x_n(1,j-1)),$$

$$x_{n+1}(i,j)=\left(1-\frac{\varepsilon_1+\varepsilon_2}{2}\right)f(x_n(i,j))+\frac{\varepsilon_1}{2}f(x_n(i-1,j))$$

$$+\frac{\varepsilon_2}{2}f(x_n(i,j-1)),\quad i,j>1$$

$$x_n(1,1)=s_n. \tag{4.1}$$

An external injection is applied to the site $i=j=1$, and it influences other sites through the couplings, acting in one direction from small i, j to large i, j. The OCOML can be modified to an OCRML system by eliminating injection and requiring a periodic boundary condition such as

$$z_{n+1}(i,j)=\Phi(z_n(i,j),z_n(i-1,j),z_n(i,j-1)),$$

$$L\geq i\geq 1,\quad N\geq j\geq 1, \tag{4.2}$$

$$z_n(1,1)=z_n(L,N),$$

where the function Φ takes exactly the same form as Eqs. (4.1). Direct numerical simulations show that at $a=4$ the state of Eqs. (4.2) is fully developed spatiotemporal chaos in almost all couplings in the range $1>\varepsilon_1>0$, $1>\varepsilon_2>0$, $1>(\varepsilon_1+\varepsilon_2)/2>0$. The desirable properties, which exist in 1D OCOML and are of crucial importance for chaos synchronization, can be easily proven to exist in the 2D case also. Specifically, we have the following.

(1) All solutions of Eqs. (4.2) are also the solutions of Eqs. (4.1) if we drive Eq. (4.1) by $x_n(1,1)=s_n=z_n(1,1)$.

(2) As $\varepsilon_1,\varepsilon_2,(\varepsilon_1+\varepsilon_2)/2>0.75$ the 2D OCOML system has only a unique asymptotic solution. If we use s_n

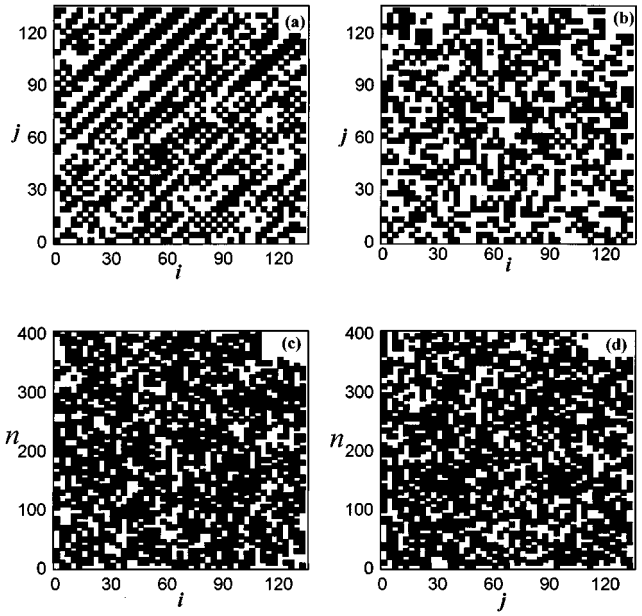

FIG. 7. Simulations of Eqs. (4.1) by certain drivings. $a=4$, $\varepsilon_1=0.95$, $\varepsilon_2=0.99$. Pixels are painted black as $x_n(i,j)>0.75$ while left blank otherwise. (a) Constant driving $s_n=0.2$ is applied to Eqs. (4.1). Frozen spatial chaos is observed. (b)–(d) Various projections of spatiotemporal chaos of (4.1). Chaotic driving is obtained from Eqs. (4.2) with $L_1=L_2=135$, $x_n(1,1)=s_n=z_n(1,1)$. (b) A snapshot of spatial pattern at $n=300$. (c) The asymptotic state at $j=30$. (d) The asymptotic state at $i=30$.

$=z_n(1,1)$ as the driving force, the solution of Eq. (4.2) is the unique attractor of Eqs. (4.1) for arbitrary initial conditions, no matter whether this solution is stable or unstable for Eqs. (4.2).

(3) For any periodic driving $s_{n+l}=s_n$, the asymptotic motions ($n\gg 1$) of all sites for $\varepsilon_1,\varepsilon_2,(\varepsilon_1+\varepsilon_2)/2>0.75$ have the same period $x_{n+l}(i,j)=x_n(i,j)$, $i,j\geqslant 1$, while various complicated spatiotemporal patterns and spatial chaos may appear, according to the particular values of s_n.

In Fig. 7(a) we plot the asymptotic state of Eqs. (4.1) by taking $a=4$, $\varepsilon_1=0.95$, $\varepsilon_2=0.99$ and using constant injection $s_n=0.2$. We get a two-dimensional frozen (time-independent) spatially chaotic pattern, which is an attractor for arbitrary initial conditions. (Here by frozen spatial chaos we mean a stable stationary state of a spatiotemporal system, whose spatial behavior is chaotic with respect to space variables.) In Figs. 7(b)–7(d), we plot various projections of a spatiotemporal chaos of Eqs. (4.1), which is produced as follows. We run Eqs. (4.2) with $L=N=135$ from a random initial condition by taking $a=4$, $\varepsilon_1=0.95$, $\varepsilon_2=0.99$, and then take $s_n=z_n(1,1)$ as the injection to drive Eqs. (4.1) with the same a and ε from another also random initial condition. After neglecting transient data, we get a spatiotemporal chaos exactly the same as that of Eqs. (4.2) in the site region $135\geqslant i,\ j\geqslant 1$. Therefore, predictable two-dimensional spatiotemporal chaos can be produced in system (4.1) by using a single driving; this observation will be extremely useful for the applications.

By using the spatiotemporal chaos of a 2D system, we can also successfully perform multichannel secure communication. Actually 2D OCOML has a very useful advantage over the 1D one. The transient time needed for the former is considerably smaller than that of the latter for the same transmission channels; that is of practical importance in actual communication. The concrete schemes of secure communications for 2D and 1D systems are similar; we will not go further in this direction. Instead, we will come to the topic of information storage by using 2D OCOML systems. In recent years, the topic of secure communication by applying chaos synchronization has been extensively investigated. A related problem of information storage, specifically, informative pattern storage, has not been considered so far. In certain situations it is necessary to keep some given patterns secure. For instance, Figs. 8(a) and 8(b) are two pictures that should be masked; they can be kept safely secret from all people except those who have the key for unmasking. A reasonable idea is to use spatiotemporal chaos for masking the pictures, and to use synchronization of chaos for the information recovering. Let us discuss two different ways to do so.

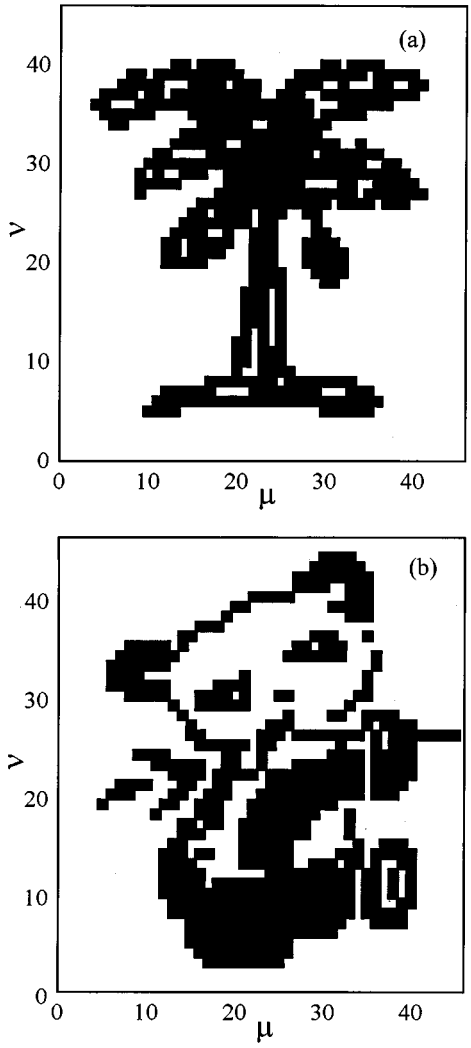

FIG. 8. Two informative patterns, which will be stored in a secure way in Figs. 9, 10, and 11. Pictures are painted in 135 $\times$135 sites; each unit of painting occupies 3×3 sites.

First, we show how to use the frozen spatial chaos of Fig. 7(a) for storing the informative picture, Fig. 8(a). Figures 8(a) and 8(b) are painted in a square of 135×135 sites to white or black in 45×45 unit blocks. Each painting unit

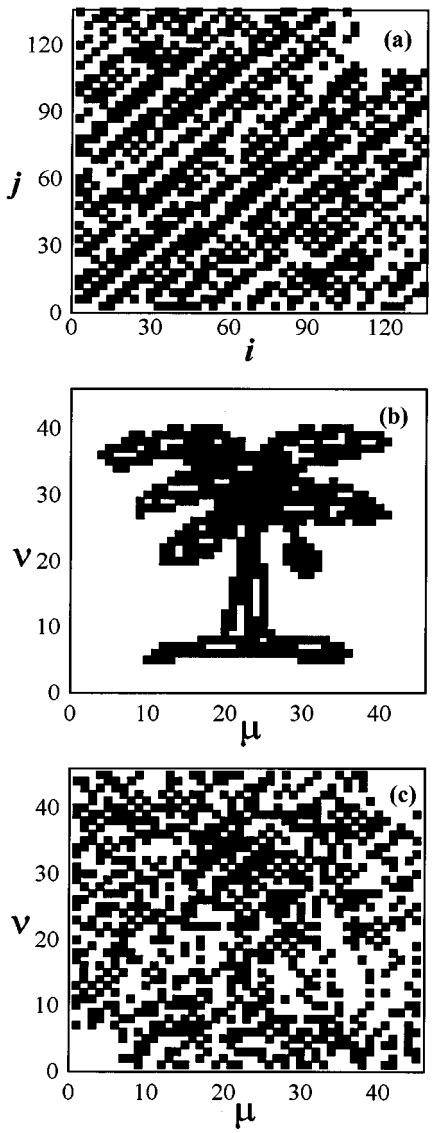

FIG. 9. (a) Figure 8(a) is masked by the frozen spatial chaos of Fig. 7(a) through Eqs. (4.4). The pixels are painted in the same way as Fig. 7(a). (b) Informative picture 8(a) is entirely recovered by Eq. (4.6). (c) By changing the driving constant to $y(1,1)=z(1,1)+10^{-6}=x(1,1)+10^{-6}$, no trace of Fig. 8(a) can be observed.

consists of $3\times3=9$ sites. We digitize the picture as

$$I[\mu(i),\nu(j)]=\begin{cases}0.02, & \text{black}\\ -0.02, & \text{white}.\end{cases} \tag{4.3}$$

Additionally, we add noise $\Gamma(i,j)$ to each site independently, which is uniformly distributed in the range $[-0.03,0.03]$. We add informative data I and noise Γ to $x(i,j)$ in Fig. 7(a) as

$$z(i,j)=x(i,j)+I[\mu(i),\nu(j)]+\Gamma(i,j). \tag{4.4}$$

$z(i,j)$ is plotted in Fig. 9(a) in the same way as Fig. 7(a), from which no trace of Fig. 8(a) can be found. Therefore, Fig. 9(a) keeps the informative picture secretly from any one without the key sequence. Driving a system identical to Eqs. (4.1),

$$y_{n+1}(i,j)=\Phi(y_n(i,j),y_n(i-1,j),y_n(i,j-1)), \tag{4.5}$$

by $y(1,1)=x(1,1)=0.2$ [where Φ has exactly the same form as Eqs. (4.1) except replacing $x_n(i,j)$ by $y_n(i,j)$], one can recover the frozen spatial chaotic pattern asymptotically $y(i,j)=x(i,j)$ from any arbitrary initial preparations. Therefore, we can pick up the informative data by

$$\hat{I}[\mu(i),\nu(j)]=\frac{1}{9}\sum_{3\mu+1}^{3\mu+3}\sum_{3\nu+1}^{3\nu+3}[z(i,j)-y(i,j)]$$
$$\approx I[\mu(i),\nu(j)]. \tag{4.6}$$

The last approximate equality is due to the fact that the masking chaotic data are canceled by the subtraction while noises are much reduced by the average process. Now the picture is repainted according to $\hat{I}[\mu(i),\nu(j)]$; i.e., black as $\hat{I}[\mu(i),\nu(j)]>0$, white otherwise. Figure 9(b) is the picture such painted that recovers Fig. 8(a) very accurately. An interesting point is that the accuracy of the picture recovered sensitively depends on the key s_n; a very small mismatch will entirely spoil the picture information. For instance, in Fig. 9(c) we do the same as in 9(b) except slightly shifting the driving constant to $y(1,1)=0.2+10^{-6}$, the resulting picture is simply a mess rather than the beautiful tree. Then it is difficult to recover the original picture from the given masking data without knowing the exact information of the key (the probability for unmasking by random tests is less than 10^{-6}). The security can be even further enhanced by making periodic drivings. For example, we can use period-2 injection $s_1=0.3$, $s_2=0.529$, $s_{n+2}=s_n$, to drive system (4.1) and get time-period-2 spatial chaos. Then we use one space chaos for masking Fig. 8(a) and the other for masking Fig. 8(b) in the manner of Eqs. (4.3) and (4.4), and then try to recover the pictures in exactly the same way as in Fig. 9(b). In Figs. 10(a) and 10(b) we use drivings $s_1=0.3$, $s_2=0.529$, $s_{n+2}=s_n$ for the receiver, and successfully recover the pictures in Figs. 8(a) and 8(b), respectively. In Figs. 10(c) and 10(d), we use $s_1=0.3$, $s_2=0.529+10^{-6}$ and $s_1=0.3+10^{-6}$, $s_2=0.529$, respectively. Then, the pictures of 8(a) and 8(b) are replaced by random dots of 10(c) and 10(d). Both s_1 and s_2 should be known precisely for the successful unmasking, and in this case the probability of imitating the key by random testings is enormously reduced to less than $10^{-6}\times10^{-6}=10^{-12}$. Actually, one can never repaint the tree and the panda unless he has precise information about the key, and any external imitations of the key are hopeless. On the other hand, one can surely recover the original pictures in our computer precision with the known key. We have tried the above procedures by using two computers produced by different companies; one serves as a transmitter and the other as a receiver. A key can be sent from the transmitter to the receiver in normal ways (e.g., by e-mail or by disk transfer). All of the above picture encoding and decoding can be performed successfully.

In Figs. 9 and 10 we used spatial chaos to mask informative pictures, where information is stored in spatial data. We can also use spatiotemporal chaos for masking and storing pictures; then the information of pictures is kept in time sequences. The approach is similar to that of multichannel

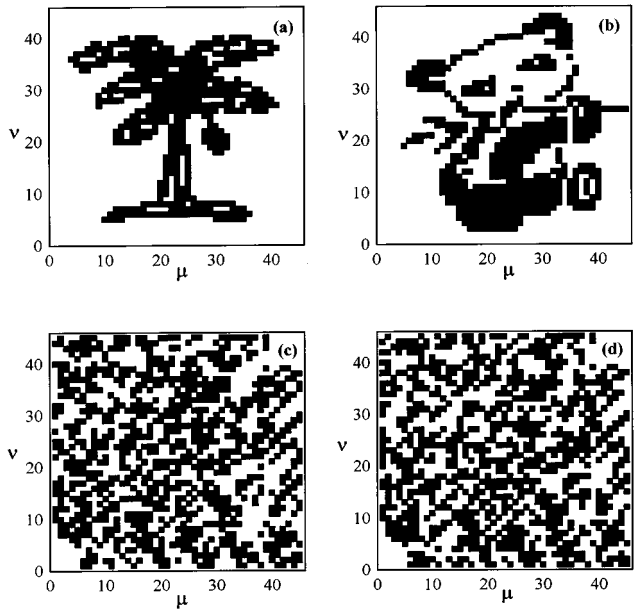

FIG. 10. (a), (b) Figures 8(a) and 8(b) are masked by the time period-2 spatial chaos, and recovered through Eq. (4.6) (driving is $s_1=0.3$, $s_2=0.529$, $s_{n+2}=s_n$). (c) The same as in (a) with the driving changed to $s_1=0.3+10^{-6}$, $s_2=0.529$. (d) The same as in (b) with the driving replaced by $s_1=0.3$, $s_2=0.529+10^{-6}$. In both (c) and (d) no trace of Figs. 8(a) and 8(b) can be found.

communication by synchronizing spatiotemporal chaos. For this purpose we digitize the picture [e.g., Fig. 8(b)] as

$$M[\mu,\nu]=\begin{cases}1, & \text{black}\\ -1, & \text{white.}\end{cases} \tag{4.7}$$

Now we use the spatiotemporal chaos of Fig. 7(b) to show how the approach works. First, all data $x_n(i,j)$ are digitized and quantized as Eq. (3.3) to $S_{n(k)}(i,j)$. Then, the chaotic sequences of all sites are modulated by Eq. (4.7) and summed as

$$G_{n(k)}=\frac{1}{45^2}\sum_{\mu=1}^{45}\sum_{\nu=1}^{45} S_{n(k)}(i=3\mu+1,\ j=3\nu+1)M[\mu,\nu], \tag{4.8}$$

$$n=1,2,\ldots,T.$$

A part of the time series $G_{n(k)}$ is given in Fig. 11(a). For information recovering, the key $s_n=x_n(1,1)$ should be given to ones who have the right to unmask the picture. The key sequence s_n should be a bit longer than T for passing the transient process. One can achieve synchronization of spatiotemporal chaos by running Eqs. (4.5), and obtaining $y_n(i,j)\approx x_n(i,j)$ and $\hat{S}_{n(k)}(i,j)\approx S_{n(k)}(i,j)$, $n=1,2,\ldots,T$. Then we can extract the masked information by the correlation checking of $G_{n(k)}$ as

$$\hat{M}[\mu,\nu]\propto\sum_{n=1}^{T}\sum_{k=1}^{J} G_{n(k)}\hat{S}_{n(k)}(i=3\mu+1,\ j=3\nu+1). \tag{4.9}$$

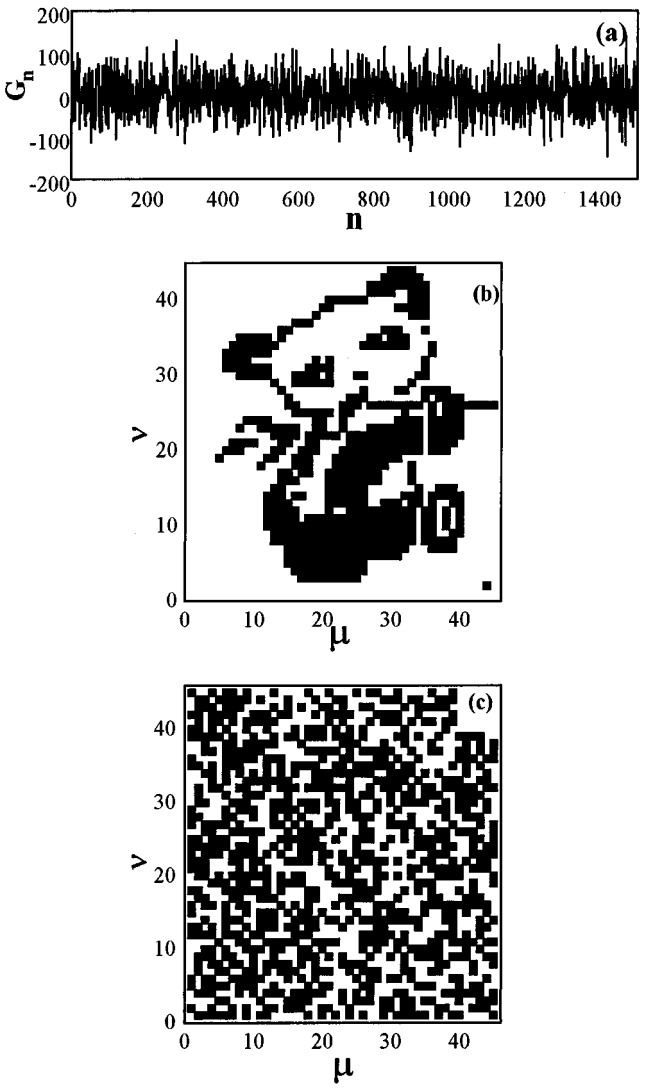

FIG. 11. Storing a spatial pattern by a time sequence. (a) The mixture of 45×45 chaotic sequences modulated by the informative picture 8(b) according to Eqs. (4.7) and (4.8). (b) Picture recovered by the correlation checking operation Equation (4.9) with $T=1500$, $J=10$. (c) The same as (b), but the driving s_n' is extracted from Eqs. (4.2) with initial condition the same as that producing Fig. 7(b) except modifying the initial value of a single site $i=30$, $j=40$ to $z_0'(20,30)=z_0(20,30)+10^{-6}$. Now no panda can be observed.

The picture can be repainted to black for $\hat{M}[\mu,\nu]>0$ and white for $\hat{M}[\mu,\nu]<0$. In Fig. 11(b) we use $T=1500$ and $J=10$, and exactly recover the picture. From the random time data of Fig. 11(a), one can hardly imagine that the complicated picture can be found. It is again emphasized that imitation of the key by random testings is absolutely impossible. For instance, we run Eqs. (4.2) by using the initial conditions, from which the spatiotemporal chaos of Fig. 7(b) is produced, except modifying the initial value of a single site, $i=20$, $j=30$, to $z_0'(20,30)=z_0(20,30)+10^{-6}$. Then we use $s_n'=z_n'(1,1)$ for unmasking the informative picture by repeating the procedures producing Fig. 11(b). Finally, we get Fig. 11(c), which is nothing but a mess. Note that the difference

between 11(b) and 11(c) is caused by a 10^{-6} difference in the initial value of a single site among the 135×135 sites. This extremely small defect leads to entire loss of information, which is really striking and interesting.

V. CONCLUSION

In conclusion, we would like to emphasize the great application potential of control and synchronization of spatiotemporal chaos. In a spatially coupled system, there may be a huge number of uncorrelated [in the sense of Figs. 3(b) and 3(c)] chaotic sites available for information operations. All these sites can be controlled in a simple way (in our case, by driving a single site among ten of thousands of sites). The parallel and simultaneous operations of these subunits may greatly enhance the efficiency of information treatments. In addition, a brief remark on data suppression and release in our systems may be useful. In Secs. III and IV we dealt with synchronization of chaotic motions in extended systems, where all data of time variations of a large number of space sites are suppressed to the key sequence representing the motion of only a single site. By using this single key and a simply spatiotemporal dynamics one can release the suppressed data, i.e., one can exactly recover the time variations of all sites. For instance, in the motion of Fig. 7(b) there are $135\times135>10^4$ chaotic sequences containing a huge number of uncorrelated motions (or say irreducible data sequences). It is interesting that all these sequences can be suppressed to the data of a single driving sequence. The suppressed data can be released by running simple nonlinear spatiotemporal dynamics driven by this key sequence, since the motions of all sites are entirely controllable (though they look madly chaotic and uncorrelated). In order to keep $135\times135N$ data we need to store only N data, which is 10^{-4} less. This function of data suppression and release may have great potential in future applications of information treatment. Nevertheless, we should emphasize that here we perform data suppression in autonomous systems. It is interesting to go further in this line to consider informative signal suppression and release by using a chaos synchronization technique; we plan to try this in our future works.

ACKNOWLEDGMENT

This work was supported by the National Natural Science Foundation of China and Nonlinear Science Project.

[1] E. Ott, C. Grebogi, and J. A. Yorke, Phys. Rev. Lett. **64**, 1196 (1990).
[2] L. M. Pecora and T. L. Carroll, Phys. Rev. Lett. **64**, 821 (1990).
[3] W. L. Ditto, S. N. Rausco, and M. L. Spano, Phys. Rev. Lett. **65**, 3211 (1990).
[4] E. A. Jackson and A. Hubler, Physica D **40**, 407 (1990).
[5] E. R. Hunt, Phys. Rev. Lett. **67**, 1953 (1991).
[6] R. Roy, T. W. Murphy, T. D. Maier, Z. Gills, and E. R. Hunt, Phys. Rev. Lett. **68**, 1259 (1992).
[7] L. O. Chua, L. Kocarev, K. Eckert, and M. Itoh, Int. J. Bifurcation Chaos Appl. Sci. Eng. **2**, 705 (1992).
[8] K. M. Cuomo and A. V. Oppenheim, Phys. Rev. Lett. **71**, 65 (1993).
[9] L. Kocarev and U. Parlitz, Phys. Rev. Lett. **74**, 5028 (1995).
[10] G. Chen, IEEE Trans. Circuits Syst. **40**, 829 (1993).
[11] W. X. Ding, H. Q. She, W. Huang, and C. X. Yu, Phys. Rev. Lett. **72**, 96 (1994).
[12] M. Ding and E. Ott, Phys. Rev. E **49**, 945 (1994).
[13] Y. C. Lai and C. Grebogi, Phys. Rev. E **49**, 1094 (1994).
[14] G. Hu and K. F. He, Phys. Rev. Lett. **71**, 3794 (1993).
[15] G. Hu and Z. L. Qu, Phys. Rev. Lett. **72**, 68 (1994).
[16] D. Auerbach, Phys. Rev. Lett. **72**, 1184 (1994).
[17] I. Aranson, H. Levine, and L. Tsimring, Phys. Rev. Lett. **72**, 2561 (1994).
[18] F. Qin, E. Wolf, and H. Chang, Phys. Rev. Lett. **72**, 1459 (1994).
[19] G. A. Johnson, M. L. Locher, and E. R. Hunt, Phys. Rev. E **51**, R1625 (1995).
[20] G. Hu, Z. L. Qu, and K. F. He, Int. J. Bifurcation Chaos Appl. Sci. Eng. **5**, 901 (1995).
[21] J. H. Xiao, G. Hu, and Z. L. Qu, Phys. Rev. Lett. **77**, 4162 (1996).
[22] K. Kaneko, Physica D **68**, 299 (1993).
[23] F. H. Willeboordse and K. Kaneko, Phys. Rev. Lett. **73**, 533 (1994).
[24] H. Dedieu, M. P. Kennedy, and M. Hasler, IEEE Trans. Circuits Syst. **40**, 634 (1993).
[25] T. L. Carrol, J. F. Heagy, and L. M. Pecorra, Phys. Rev. Lett. **76**, 904 (1996).
[26] U. Parlitz and S. Ergezinger, Phys. Lett. A **188**, 146 (1994).
[27] R. E. Ziemer and R. L. Peterson, *Digital Communications and Spread Spectrum Systems* (Macmillan Publishing Company, New York, 1985).
[28] G. Heidari-Bateni and C. D. McGillem, IEEE Trans. Commun. Technol. **2/3/4**, 1524 (1994).